Purdue University Purdue e-Pubs

ECE Faculty Publications

Electrical and Computer Engineering

2009

A linear programming approach to shipboard electrical system modeling

Ricky R. Chan

Scott D. Sudhoff

Yonggon Lee

Edwin L. Zivi

Follow this and additional works at: http://docs.lib.purdue.edu/ecepubs

Chan, Ricky R.; Sudhoff, Scott D.; Lee, Yonggon; and Zivi, Edwin L., "A linear programming approach to shipboard electrical system modeling" (2009). *ECE Faculty Publications*. Paper 38. http://dx.doi.org/http://dx.doi.org/10.1109/ESTS.2009.4906524

This document has been made available through Purdue e-Pubs, a service of the Purdue University Libraries. Please contact epubs@purdue.edu for additional information.

A Linear Programming Approach to Shipboard Electrical System Modeling

Ricky R. Chan and Scott D. Sudhoff School of Electrical and Computer Engineering Purdue University West Lafayette, IN, USA Yonggon Lee and Edwin L. Zivi Weapons and Systems Engineering U.S. Naval Academy Annapolis, MD, USA

Abstract—Operability and dependability metrics can be a valuable tool in early ship design by providing a quantitative analysis of the robustness of the ship's integrated engineering plant (IEP). However, the use of these metrics involves large numbers of time domain simulations of the IEP. The simulation of such a complex system, which includes electrical and thermal subsystems, can be problematic in terms of computational efficiency. In this paper, a simplified modeling approach based on the fundamental power limitations is set forth. The power flow problem is posed as a linear programming problem which is solved using a simplex method.

I. INTRODUCTION

Warfighting capability following a hostile disruption is clearly important in the early design stage of an electric warship. The integrity of the ship integrated engineering plant (IEP) is key to maintaining warfighting capability. A shipboard integrated engineering plant (IEP) provides engineering services such as electrical power and coolant [1]. In order to measure and quantify the performance of an IEP against a disturbance, system performance metrics have been proposed [2]–[5]. Examples of the metrics include the operability and dependability. In particular, the operability and the dependability metrics measure to what degree engineering services are provided to system loads following a hostile disruption [2]. In an electric warship, the loads include propulsion systems, radar, weapon systems, as well as communication systems.

Prior to further discussion regarding these metrics, it is appropriate to first introduce the notion of event θ . An event $\theta \in \Theta$ is a vector whose elements describe a disruption to a ship. For example, θ may consist of the coordinates and radius of the weapon detonation. A more detailed description of the event is set forth in [2]. In this work, Θ denotes a set of all possible events. The operability metric considers a set of all possible events. The operability metric considers a set of all possible events. The operability metric is formulated as

$$O(\theta) = \frac{\int_{t_0}^{t_f} \sum_{i=1}^{I} w_i(t, \theta) o_i^*(t) o_i(t) dt}{\int_{t_0}^{t_f} \sum_{i=1}^{I} w_i(t, \theta) o_i^*(t) dt}$$
(1)

where $w_i\left(\cdot,\cdot\right)$, $o_i^*(t)$, and $o_i(t)$ denote the relative weight factor, the commanded operational status and the operational status of the i'th load. In (1), t_0 denotes the time when the event occurs and t_f denotes the time at which interesting behavior ends.

Whereas the operability metric is focused on a specific event, the dependability metric considers all possible events. The minimum and average system dependability are defined as

$$D_{s,min} = \min_{\theta \in \Theta} O\left(\theta\right) \tag{2}$$

and

$$\bar{D}_{s} = \int_{0}^{\infty} O(\theta) \, \rho(\theta) \, d\theta \tag{3}$$

In (3), ρ denotes the probability density function of the event. Evaluation of the dependability metrics in (2)-(3) requires 10^3 - 10^6 time-domain simulations of the IEP. A complicating feature of the simulation is that they include both the slow thermal dynamics of the cooling plant as well as the much faster dynamics of the electrical plant, resulting in a numerically stiff system model. Although ordinary differential equation (ODE) solvers are available for numerically stiff systems, they invariably require adjustments in terms of time step settings. These settings must be adjusted depending upon the parameters of the system. Clearly this is not feasible to be done manually given the number of simulations being conducted.

In this paper, an electrical system modeling approach is proposed to circumvent this problem. This method focuses on the fundamental power limitations without considering waveform level details. As a result, studies can be made prior to the development of the detailed control strategies or component designs being available. Interactions between electrical components are represented in terms of power. This approach assumes that all devices are appropriately controlled. To this end, power distribution of the electrical system is formulated as a linear programming problem [6]. A simplex method is utilized to determine the power flow as an alternative to direct simulation of the electrical dynamics. This approach to reduced-order modeling not only represents the system dynamics but also provides an optimal control strategy.

It must be recognized that the level of details provided by this approach is much less than that of traditional simulation. However, it can be used before the design details needed for a detailed simulation are available. It is an appropriate approach for early ship design studies in the context of operability and dependability metrics. This approach is not a replacement for a traditional system representation when detailed system information is available and a modest number of runs are required.

This paper will be organized as follows. First, a notional integrated engineering plant (IEP) is described in Section II. In Section III, the electrical system modeling approach as a linear program is set forth. The detailed algorithm to solve this problem is set forth in Section IV. Section V provides a detailed explanation on the electrical component models. Section VI presents a scenario to illustrate the proposed approach as well as the results obtained. This section also includes a comparative study between the proposed modeling approach and a more detailed approach. This paper concludes with a summary and recommendations for future work in Section VII.

II. INTEGRATED ENGINEERING PLANT

An integrated engineering plant (IEP) provides critical engineering services to all shipboard loads. Since the electrical system requires the shipboard freshwater and seawater cooling system and the seawater and freshwater components require electrical power, the thermal and

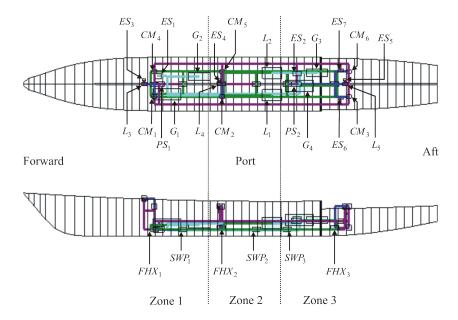


Fig. 1. Notional Layout of IEP.

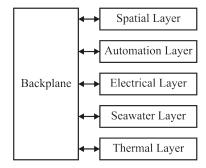


Fig. 2. Layered Approach.

electrical systems are highly coupled. The notional layout of the example IEP is depicted in Fig. 1. Therein, ES denotes an energy storage unit, CM denotes a dc-dc converter module, PS denotes a power supply (ac-dc converter), G denotes a generator, L denotes a load, FHX denotes a fluid heat exchanger, and SWP denotes a seawater pump unit. A layered approach in Fig. 2 was proposed in [2] to model the IEP. Each layer has a clearly defined inputs and outputs from the other layers. This approach allows flexibility in the case when additional layers are needed. In this paper, the electrical layer remains the focus of the work. Other layers will be briefly discussed.

A. Spatial Layer

The spatial layer represents the components as geometrical objects. In particular, the spatial layer represents electrical components and pumps as rectangular prisms. The electrical connections and piping are represented as lines. Using this representation, the spatial effect of missile detonation on the components can be determined in terms of the hit status h. A detailed IEP component placement within the ship is set forth in [2].

B. Automation Layer

The automation layer consists of supervisory controllers. This control determines when to activate or deactivate the associated device. To this end, the operational status

$$o := \alpha + \bar{\beta}o \tag{4}$$

is assigned for each component, where α denotes the activation signal, β denotes the deactivation signal, and "+" denotes a logical OR operation. In (4), ":=" denotes an assignment operator.

1) Generator Supervisory Control: The generator supervisory signals are assumed to be given by

$$\alpha = o^* \bar{h} \bar{o}_h \left(P_{load} \ge P_{min} \right) \left(P_{load} \le P_{max} \right) \tag{5}$$

$$\beta = \bar{o^*} + h + o_h + (P_{load} < P_{min}) + (P_{load} > P_{max})$$
 (6)

where o^* denotes the commanded operating status, h denotes the hit status, o_h denotes the overheat status, P_{load} denotes the loading power, P_{max} and P_{min} denote the instantaneous maximum and minimum power capability, respectively.

In this work, the overheat status is formulated as

$$o_h := o_h + (T > T_{max}) \tag{7}$$

where T_{max} denote the maximum operating temperature of the generator. To this end, the generator operational status can be determined using (4).

2) Converter and Load Supervisory Control: The converter and load supervisory controls are similar and they are governed by the following activation and deactivation signals

$$\alpha = o^* \cdot \bar{h} \cdot \bar{o}_h \tag{8}$$

$$\beta = \bar{o^*} + h + o_h \tag{9}$$

The converter and load overheat determination is similar to (7). However, note that T_{max} is a function of the specific component

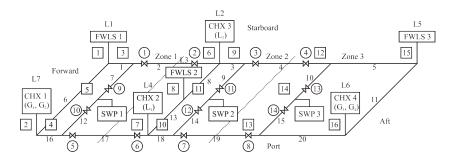


Fig. 3. Seawater Network.

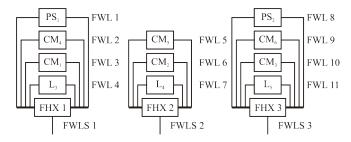


Fig. 4. Freshwater Loops.

being considered. To this end, the converter and load operational status can be determined using (4).

3) Energy Storage Unit Supervisory Control: It is assumed herein that the energy storage units do not require an external thermal management and that they are always commanded to be operational. With these assumptions, the supervisory control is only a function of hit status, expressed as

$$\alpha = \bar{h} \tag{10}$$

$$\beta = h \tag{11}$$

The energy storage unit operational status is also determined using (4). Note that simply being operational is not a sufficient condition for the energy storage unit to be able to provide power to the system. This requires a sufficient amount of energy to be stored in addition to being operational.

C. Seawater Layer

The seawater layer contains the models of the components in the seawater network, such as pumps and valves. The seawater network is configured in a zonal like architecture to provide system robustness, as depicted in Fig. 3. Herein, seawater is used to provide cooling for the larger electrical components, such as the generators and the propulsion systems, as well as the freshwater loops via the fluid heat exchangers (FHX). The seawater network solver is set forth in [2].

D. Thermal Layer

The thermal layer contains the models for the fluid heat exchangers and the freshwater loops. In this work, the freshwater loops are used to cool smaller power electronics components, such as the power converters and zonal loads. The freshwater loops are depicted in Fig. 4. The complete models for the component heat exchangers and the freshwater loops are set forth in [2].

III. ELECTRICAL SYSTEM MODELING

In this work, the electrical system modeling approach is of primary interest. The approach herein focuses on fundamental power limitations rather than waveform level details. The intent is for an analysis that can be used in the early design stage before the details of the control and the components are known. In this stage of the design, issues such as component layout within the ship so as to facilitate high dependability are being considered. This approach to reduced-order modeling is advantageous in that it represents both the system dynamics as well as provides an optimal control strategy.

The one line diagram of the electrical system of the notional IEP is depicted in Fig. 5. In the electrical system, an ac system is considered to include four generators $(G_1$ through G_4), two ac loads $(L_1$ and L_2), as well as two energy storage units $(ES_1$ and ES_2). In this work, the ac loads represent the propulsion systems.

The electrical system also consists of a dc system, where the dc system is configured into a zonal like architecture [8]. In particular, the dc system consists of three identical dc zonal systems. In each zone, two dc-dc converters (C_1 through C_6), one energy storage unit (ES_3 through ES_5) and a dc load (L_3 through L_5) are considered. In addition, two energy storage units (ES_6 and ES_7) are allocated in the dc distribution busses; one on the port side distribution bus and the other on the starboard side.

In the proposed electrical system modeling approach, the dc-dc converters and the power supplies are modeled as a general power converter and thus is denoted as C_1 through C_8 in Fig. 5. In the notional system, C_1 through C_6 are dc-dc converter modules while C_7 and C_8 are ac-dc power supplies.

In Fig. 5, lines denote electrical connections. Each line contains a directional arrow to indicate the direction of power flow and is denoted with \hat{x}_1 through \hat{x}_{51} , where \hat{x}_i denotes the power allocated in the i'th line. Note that several electrical lines in Fig. 5 contain two directional arrows in the opposite direction. The linear program and simplex method, which will be described shortly, do not allow negative power allocations and thus two power allocations are required to represent bidirectional power flows.

The power distribution problem is now posed as a linear programming problem. The objective is to determine the power distribution that yields the maximum power allocation to the loads. Recall that the proposed method is intended for early design studies before detailed controls or components parameters are known. The assumption is that when the detailed components controls are designed, they will be designed so as to approximately achieve the optimal power flow performance.

Thus, this simulation methodology reflects what is possible to achieve, since it is assumed that the detailed control strategy is not available at this point in the design process. Henceforth, the proposed

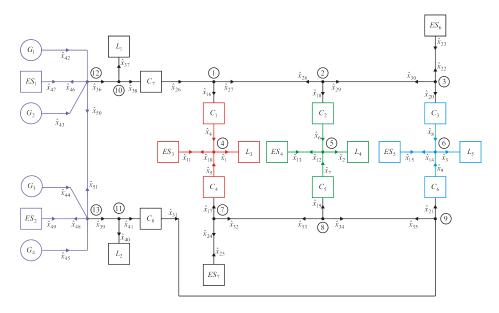


Fig. 5. Electrical System of the Notional IEP.

method will be referred to as the \underline{L} inear \underline{P} rogramming \underline{P} ower \underline{S} ystem \underline{S} imulation (LPPSS) approach.

A simplex method has been chosen to solve the linear program to obtain the optimal power distribution [6], [7]. The use of the linear program and simplex method to determine the optimal power allocation provides an alternative approach to direct simulation of the electrical system.

One of the key challenges in using linear programming in this context is to ensure proper load sharing among power sources. At first, it would seem that this could be readily addressed through the use of equality constraints, which are a standard part of the linear program. However, the situation is more subtle than this because sharing does not always result in a power distribution which maximizes the portion of the load demand satisfied.

When all components of the notional IEP are operational in steadystate, it is expected that power sharing among all generators will result in the maximum power allocations to the loads. However, following a disruptive event where parts of the architecture are compromised, it may not be optimal or physically possible to fully achieve power sharing.

For example, in Fig. 5, suppose that the line between bus 12 and bus 13 is severed. Then it is unreasonable to suppose that the set of generators $\{G_1G_2G_3G_4\}$ will share load. However, it is reasonable that the set $\{G_1G_2\}$ will share load and the set $\{G_3G_4\}$ will share loads. The configuration of generator sharing load will be referred to as the sharing scenario. For example, the scenario $\{G_1G_2G_3G_4\}$ means that all generators are sharing while the scenario $\{G_1G_2\},\{G_3G_4\}$ means that G_1 and G_2 are sharing and G_3 and G_4 are sharing. However the two sets are not sharing as aggregates. While the present discussion has focused on generator sharing, zonal sharing scenario between the various converter modules must also be considered. Thus, in order to guarantee maximum power allocation to the load, all possible scenario combinations must be considered.

At this point, the problem may be formulated mathematically as

maximize
$$\mathbf{c}^{\mathrm{T}}\hat{\mathbf{x}}$$

subject to $\mathbf{A}_{1}\hat{\mathbf{x}} \leq \mathbf{b}_{1}$
 $\mathbf{A}_{2}\hat{\mathbf{x}} \geq \mathbf{b}_{2}$ (12)
 $\mathbf{A}_{3}\hat{\mathbf{x}} = \mathbf{b}_{3}$
 $\hat{\mathbf{x}} > 0$

The formulation of the linear program in (12) corresponds to the form required by the simplex method in [7]. In (12), $\mathbf{c}^T\hat{\mathbf{x}}$ denotes the objective function with \mathbf{c} as the weight matrix while $\mathbf{A_1}\hat{\mathbf{x}} \leq \mathbf{b_1}$, $\mathbf{A_2}\hat{\mathbf{x}} \geq \mathbf{b_2}$, $\mathbf{A_3}\hat{\mathbf{x}} = \mathbf{b_3}$, and $\hat{\mathbf{x}} \geq 0$ indicate the constraints that must be satisfied.

The objective function is formulated to maximize power allocation to the loads and to encourage the energy storage units to charge when possible. Recall that each element of $\hat{\mathbf{x}}$ corresponds to the power flow in a line. The power flow in a unidirectional line corresponds to a single element of $\hat{\mathbf{x}}$ and the power flow in a bidirectional line corresponds to two elements of $\hat{\mathbf{x}}$ - one element for power flow in both directions.

Each element of c weighs the power flow with the corresponding element of \hat{x} . Thus, the strategy for constructing the objective function is to assign positive value to those elements of c corresponding to power flow into loads. The relative value of those elements determines the relative weight of the load.

In addition, those elements of c corresponding to the power flow into the energy storage units are given low positive weights to encourage charging when power is available. Elements corresponding to power delivery from energy storage units are given small negative weights; thus preventing the units from discharging unless they are needed to satisfy the load demand. The selection of the weight matrix c for the nominal system is listed in Table IV in the Appendix.

Recall that every feasible load sharing scenario must be investigated to determine the optimal solution. To accomplish this feature, an iterative LPPSS algorithm is set forth in Section IV. This algorithm considers every combination of N_{GSS} generator sharing scenarios and N_{ZSS} zonal sharing scenarios. The generator and zonal sharing scenarios are itemized in Table I and Table II. In Table II, a one

(zero) indicates the converter modules within the zone are (are not) sharing.

The number of the inequality constraints is constant and a function of the number of lines in the electrical system representation. However, the number of equality constraints varies as a function of the number of busses in the electrical system representation, the converter input-output power constraints, and the generator and zonal power sharing.

In Section IV, all feasible generator and zonal sharing scenarios are considered. To be feasible, all equipment needed for a given operational scenario must be available. For example, if G_1 is not operational, then the sharing set $\{G_1G_2G_3G_4\}$ is not feasible - and nor is any other scenarios that involves power sharing with G_1 . At the end of Algorithm 1, a maximum of $N_{GSS}N_{ZSS}$ potential power flow solutions are obtained. The selection of the actual final solution from among the potential solutions is the final step of the algorithm.

IV. LPPSS ALGORITHM

The LPPSS algorithm is as follows:

- Step 1 Less-than Constraints. The first step in the algorithm is to construct the less-than constraints according to the formulation of the linear program in (12). In the context of the electrical system, this constraint provides an upper limit on the power that can be allocated on the line. In this work, $\mathbf{A_1} = \mathbf{I_n}$ and $\mathbf{b_1} \in \mathbb{R}^n$ represents a vector of the power allocation upper bounds, where n denotes the number of electrical lines.
- Step 2 Greater-than Constraints. The second step of the algorithm is to construct the greater-than constraints. Herein, the greater-than constraints are required to provide the lower bounds on the power allocations. Although the use of the simplex algorithm in [7] already governs that the solutions are nonnegative, the electrical power lines connecting the generator may require the lower bounds to be greater than zero. Herein, A₂ = I_n and b₂ ∈ Rⁿ represents a vector of power allocation lower bounds.
- Step 3 Equality Constraints: Conservation of Power. In the electrical system representation, a conservation of power is observed on each bus. An example is provided herein to illustrate the equality constraints obtained by observing the conservation of power on bus 10 of the electrical system in Fig. 5, such that

$$\hat{x}_{36} - \hat{x}_{37} - \hat{x}_{38} = 0 \tag{13}$$

Similar equality constraints can be constructed for the other busses.

• Step 4 - Equality Constraints: Converter Input-Output Power. In this step, the appropriate converter input-output power relationship is formulated as equality constraints. First, all operational converters are determined. For each operational converter, the output power is formulated as a function of the input power, the efficiency, and the constant no-load power loss. The input-output power relationship for an operational converter is represented using an equality constraint. An example is provided herein to illustrate the equality constraint based on the input-output power relationship of converter C_1 as

$$\hat{x}_4 - \eta_{inc}\hat{x}_{16} = \eta_{inc}P_{nl} \tag{14}$$

A more detailed derivation of the form in (14) will be described in Section V-B.

Step 5 - Outer Loop Initilization. The outer loop iteration count
 i is initialized to one.

- Step 6 Outer Loop Test. In this step, i is compared with N_{GSS}.
 If i

 N_{GSS}, then continue to Step 7. Otherwise, proceed to Step 12.
- Step 7 Generator Sharing. The feasibility of the i'th generator sharing scenario is determined in this step. If the i'th sharing scenario is feasible, then the following generator sharing scenarios can be formulated as equality constraints. Otherwise, increment i and return to Step 6. In this work, the generator sharing rules are formulated as

$$\hat{x}_i = \frac{P_{rated,i}}{P_{rated,total}} P_{load,total} \tag{15}$$

where $P_{load,total} = \hat{x}_i + \hat{x}_j + \ldots + \hat{x}_l$ denotes the sum of the load powers requested from all sharing generators, $P_{rated,i}$ denotes the rated power of each generator, and $P_{rated,total}$ denotes the sum of the rated power of all sharing generators. The sharing rule in (15) determines that sharing generators are loaded proportionally according to the rated power. Substituting the expression of $P_{load,total}$ into (15) and rearranging, the following equality constraint is obtained

Herein, k-1 equality constraints similar to (16) are required for k sharing generators to allow a feasible solution to be determined. This is due to the linear dependence of the k'th equality constraint to the previous k-1 constraints.

- Step 8 Inner Loop Initilization. Initialize the inner loop iteration count j=1.
- Step 9 Inner Loop Test. In this step, the inner loop iteration count j is compared with the number of zonal sharing scenarios N_{ZSS}. If j ≤ N_{ZSS}, then continue to Step 10. Otherwise, increment i and return to Step 6.
- Step 10 Zonal Sharing Scenarios. Evaluate the feasibility of the j'th zonal sharing scenario. If not feasible, increment j and return to Step 9. If feasible, formulate the zonal sharing scenarios as equality constraints subject to the following conditions. In a dc network with m zonal dc systems similar to the one considered in this work, there are 2^m possible zonal sharing scenarios. In the case of the notional IEP, three dc zonal systems are considered and therefore eight possible sharing scenarios are possible for the notional system, as itemized in Table II.

A zonal sharing scenario is feasible if the involved pairs of converters are operational. For example, Scenario 8 in Table II involves the converters in all three zones. However, if one of the converters is damaged, then Scenario 8 is no longer feasible. This also applies to the other scenarios that involve sharing with the damaged converter.

When two converter modules share, the allocated output powers must be equal, thus

$$\hat{x}_i - \hat{x}_j = 0 \tag{17}$$

In (17), \hat{x}_i and \hat{x}_j denotes the output powers of the sharing converters.

Step 11 - Linear Program Formulation. It is now appropriate to
formulate the linear program as described in (12). A simplex
method is utilized to determine the electrical system power
distribution. After the solution is recorded, increment the inner
loop iteration count j and proceed to Step 9.

TABLE I Notional IEP Generator Sharing Scheme

Scenario No.	Sharing Config.	Scenario No.	Sharing Config.
1	G_1, G_2, G_3, G_4	9	$G_1, \{G_2G_4\}, G_3$
2	${G_1G_2},G_3,G_4$	10	$G_1,G_2,\{G_3G_4\}$
3	$\{G_1G_2\},\{G_3G_4\}$	11	$\{G_1G_2G_3\},G_4$
4	$\{G_1G_3\},G_2,G_4$	12	$\{G_1G_2G_4\},G_3$
5	$\{G_1G_3\},\{G_2G_4\}$	13	$G_1G_3G_4$, G_2
6	$\{G_1G_4\},G_2,G_3$	14	$G_1, \{G_2G_3G_4\}$
7	$\{G_1G_4\},\{G_2G_3\}$	15	$\{G_1G_2G_3G_4\}$
8	$G_1, \{G_2G_3\}, G_4$	_	- '

TABLE II

NOTIONAL IEP ZONAL SHARING SCENARIOS

Scenario No.	Zone 1	Zone 2	Zone 3
1	0	0	0
2	0	0	1
3	0	1	0
4	0	1	1
5	1	0	0
6	1	0	1
7	1	1	0
8	1	1	1

• Step 12 - Solution Determination. In the case of the algorithm, a maximum of $N_{GSS}N_{ZSS}$ potential power flow solutions are obtained. Nominally, the solution with the largest objective function value $\mathbf{c}^{\mathrm{T}}\hat{\mathbf{x}}$ is selected as the final solution. In the event that multiple solutions have the same objective function value, a secondary objective function is used. In particular, of the solutions which share the maximum value of $\mathbf{c}^{\mathrm{T}}\hat{\mathbf{x}}$, the solution with the smallest value of

$$f_2 = \sqrt{\sum_{c=1}^{C} c_{err,c}^2 + \sum_{g=1}^{G} g_{err,g}^2}$$
 (18)

is chosen. In (18), $c_{err,g}$ denotes the error between the actual output power of the c'th converter and the output power under ideal sharing scenario. Similarly, $g_{err,g}$ denotes the error between the actual power provided by the g'th generator and the desired power under ideal sharing condition. In the case of the notional IEP, the ideal sharing scenarios involves power sharing among all four generators as well as the six zonal converters. When there is no feasible solution, a zero solution is assigned to $\hat{\mathbf{x}}$.

V. ELECTRICAL COMPONENT MODELS

Thus far, an overall approach to representing the power system power flow problem in terms of a linear program has been set forth. In the previous section, a solution to the power flow problem was set forth in terms of component power limits. The instantaneous values of these limits are determined by the components models. These components models are set forth in this section.

A. Generator Model

Herein, a highly simplified model of the generator is presented. In this model, detailed voltage and current dynamics are not considered. Instead, the power limitations of the generator are acknowledged in terms of the maximum and minimum instantaneous power capability. To this end, the dynamics of maximum and minimum instantaneous power capability are formulated as

$$pP_{max} = \text{bound}(-P_{max,sr}, P_{max,lr}, \frac{1}{\tau} (P_{max,ss} (P_{load}) - P_{max}))$$
(19)

$$pP_{min} = \text{bound}(-P_{min,sr}, P_{min,lr}, \frac{1}{\tau} (P_{min,ss} (P_{load}) - P_{min}))$$
(20)

where p denotes the Heaviside notation for the time derivative operator, $P_{max,sr}$, $P_{max,lr}$, $P_{min,sr}$, and $P_{min,lr}$ denote the maximum (or minimum) shedding and loading rate, $P_{max,ss}\left(\cdot\right)$ and $P_{min,ss}\left(\cdot\right)$ denote the steady-state maximum and minimum power, formulated as a function of the load power P_{load} . The bound $\left(\cdot\right)$ operator is defined herein as

bound
$$(l, u, y) = \begin{cases} u & \text{if } y > u \\ y & \text{if } l \le y \le u \\ l & \text{if } y < l \end{cases}$$
 (21)

where \boldsymbol{l} denotes the lower bound, \boldsymbol{u} denotes the upper bound, and \boldsymbol{y} denotes the variable to be bounded.

For the notional system, $P_{max,ss}(\cdot)$ is expressed as

$$P_{max,ss} = \begin{cases} \text{bound} (0, P_{rated}, m_{max} P_{load} + P_{nl,max}) & \text{if } o \\ 0 & \text{otherwise} \end{cases}$$

where m_{max} denotes the maximum loading factor, $P_{nl,max}$ denotes the maximum no-load power, P_{rated} denotes the rated power for the corresponding generator, and o denotes the generator operational status

In the case of the minimum instantaneous power capability, $P_{min,ss}\left(\cdot\right)$ is expressed as

$$P_{min,ss} = \begin{cases} \text{bound} \left(0, \frac{P_{rated}}{4}, m_{min} P_{load} - P_{nl,min}\right) & \text{if } o \\ 0 & \text{otherwise} \end{cases}$$
(23)

where m_{min} denotes the minimum loading factor and $P_{nl,min}$ denotes the minimum no-load power.

The power loss of the generator is computed as

$$P_{loss} = (1 - \eta) P_{load} \tag{24}$$

where η denotes the efficiency of the generator. The power loss is injected to the thermal model as the heat dissipated to the heat exchanger. The generator model parameters are listed in the Appendix.

In order to illustrate some of the properties of this model, consider a series of events that include dynamic step loading and shedding. In particular, in Fig. 6, the top trace depicts the maximum allowed loading limit P_{max} , the middle trace depicts P_{load} , and the bottom trace depicts the minimum allowed loading limit P_{min} . Therein, P_{load} represents the loading of a generator as a function of time through a series of step load changes. This changes the maximum and minimum allowed loading limit on the generator, P_{max} and P_{min} . If during this sequence of events, P_{load} has increased beyond P_{max} or less than P_{min} , the generator would go off-line using this model.

B. Converter Model

While the generator power dynamics are formulated as a function of load power, the converter model does not contain any dynamics. Instead, the converter's output power P_{out} is expressed as a function

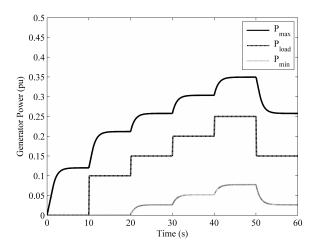


Fig. 6. Generator Modeling Example.

of the input power P_{in} , the incremental efficiency η_{inc} , and the constant no-load power loss P_{nl} as

$$P_{out} = \eta_{inc} P_{in} - P_{nl} \tag{25}$$

The efficiency and the constant no-load power loss may be unique for each converter. The power loss from the converter model is injected into the thermal model as the power dissipated to the heat exchangers, where the power loss is computed as

$$P_{loss} = (1 - \eta_{inc}) P_{in} + \eta_{inc} P_{nl}$$
 (26)

Recall that the converter model can be applied for both the dc-dc converter modules as well as ac-dc converters such as the power supplies. The converter model parameters are listed in the Appendix.

C. Load Model

In order to further simplify the electrical system, the inverter module-load bank systems in the dc zones are modeled as aggregate loads. This modeling approach therefore only considers the total load power that should be serviced at a given time. The aggregate load power $P_{L,A}$ may be formulated as

$$P_{L,A} = \sum_{i=1}^{I} (P_{L,i} + P_{L,loss,i}) o_i$$
 (27)

where $P_{L,i}$ denotes the rated power for the i'th load, o_i denotes the operational status of the associated load, and I denotes the total number of loads. In this work, the load power loss is expressed as

$$P_{loss,i} = (1 - \eta_i) P_{L,i}$$
 (28)

where η_i denotes the efficiency of the i'th load. The power loss is also injected to the thermal model as the heat dissipated to the heat exchanger of that component. The load model parameters are listed in the Appendix.

D. Energy Storage Model

Since the interactions between electrical system components are based on power distribution, the energy storage model is also formulated in terms of power. In particular, the energy storage unit will be charged when there is an available power from the system. The energy storage then provides temporary power while the system is reconfigured and power delivery to the system loads is disrupted.

Let E denotes the energy stored in the unit, the dynamics of the energy storage units is given by

$$pE = \begin{cases} -\frac{E}{\tau_{ES}} & \text{if } \bar{o} \\ 0 & \text{if } o(P_{in} > 0) (E \ge E_{max}) \\ 0 & \text{if } o(P_{out} > 0) (E \le 0) \\ \eta P_{in} - P_{nl} & \text{if } o(P_{in} > 0) (E < E_{max}) \\ -((2 - \eta) P_{out} + P_{nl}) & \text{if } o(P_{out} > 0) (E > 0) \end{cases}$$

where η denotes the efficiency of the energy storage unit, E_{max} denotes the maximum energy storage capacity, P_{in} denotes the input power, and P_{out} denotes the output power discharged into the system. In (29), P_{nl} denotes the constant no-load power loss. In the event that the energy storage unit is damaged, the energy will be discharged with time constant τ_{ES} .

Based on the state of the energy E, the energy storage model then determines the maximum charging and discharging power capability P_c and P_d , respectively, expressed as

$$P_{c} = \begin{cases} P_{c,max} & \text{if } o (E < E_{max}) \\ 0 & \text{otherwise} \end{cases}$$

$$P_{d} = \begin{cases} P_{d,max} & \text{if } o (E > 0) \\ 0 & \text{otherwise} \end{cases}$$
(30)

$$P_{d} = \begin{cases} P_{d,max} & \text{if } o(E > 0) \\ 0 & \text{otherwise} \end{cases}$$
 (31)

Using the expressions in (30) and (31), the energy storage units can be charged if there is power in the system, if they are operational, and if they are not fully charged. Similarly, the energy storage units will be discharged if power is required, if they are operational, and if they are not completely discharged. In (30) and (31), $P_{c,max}$ and $P_{d,max}$ denote the rated charging and discharging power of the energy storage unit. The values of P_c and P_d will then be used in the linear program as maximum power constraints. The energy storage model parameters are listed in the Appendix.

E. Line Model

A line is used to indicate an electrical connection between an electrical component and a bus or a connection between two busses. Based on the line type, the maximum and minimum line limits are set in accordance with

$$P_{line,max} = \begin{cases} P_{line,r} & \text{if } \bar{h} \text{ (Type} = 1) \\ \min(P_{comp,max}, P_{line,r}) & \text{if } \bar{h} \text{ (Type} = 2) \\ \min(P_{comp,max}, P_{line,r}) & \text{if } \bar{h} \text{ (Type} = 3) \\ 0 & \text{if } h \end{cases}$$
(32)

$$P_{line,min} = \begin{cases} 0 & \text{if } \bar{h} \cdot (\text{Type} = 1) \\ 0 & \text{if } \bar{h} \cdot (\text{Type} = 2) \\ \max(P_{comp,min}, 0) & \text{if } \bar{h} \cdot (\text{Type} = 3) \\ 0 & \text{if } h \end{cases}$$
(33)

where line type 1 denotes a connection between 2 busses, line type 2 denotes a connection between a load, a converter, or an energy storage unit and a bus, while line type 3 denotes a connection between a generator and a bus. In (32) and (33), h denotes the line hit status, $P_{line,r}$ denotes the maximum line power rating, $P_{comp,max}$ denotes the maximum power of the component where the line is connected, and $P_{comp,min}$ denotes the minimum power of the component where the line is connected. For the studies to be presented, $P_{line,r} = 1.0$ pu.

VI. RESULTS

The mathematical models of the IEP and the linear programming technique have been set forth in the previous chapter. This section continues with an example study using the proposed modeling approach to explore the performance of the notional IEP using the system metrics set forth in (1)-(3) are used to quantify the performance of the IEP.

A. Example Study

In order to demonstrate the proposed approach, the calculation of the operability for a disruptive event will be considered. The system is initially in the steady state with all components operational. The loads are provided maximum power and the energy storage units are charged to the maximum capacity E_{max} . At this point, load powers are distributed proportionally among all generators. Zonal converter modules also share the zonal load power. Then, at $t=300~{\rm s}$, a disruptive event, represented as a spherical blast with a radius of $r=2.0~{\rm m}$, centered at $(x_d,y_d,z_d)=(50.0,0.0,4.0)$ in the Cartesian coordinates, occurs. This particular explosion damages generator G_1 , seawater pump SWP_1 , the electrical power connection to SWP_1 , and seawater branches 7 and 12 (SWB_7) and SWB_{12} .

From the simulation, the propagation of a cascading failure can be traced. After the explosion, G_1 is no longer operational. However, the IEP can be reconfigured such that load powers are distributed to the other generators to preserve power delivery to the loads. The damage to SWP_1 causes the fluid heat exchanger FHX_1 and the freshwater loops $FWLS_1$ to lose their cooling source. The loss of coolant results in the shutdown of C_1 and C_4 at $t \approx 352$ s. In Fig. 7, the temperatures of C_1 and C_4 are depicted by traces labeled T_{FWL2} and T_{FWL3} , which corresponds to the temperature of the freshwater cooling loops of C_1 and C_4 respectively. Meanwhile, C_7 remains operational to distribute power to the zonal system via the port side distribution bus until it overheats at $t \approx 404$ s, as depicted by the trace labeled T_{FWL1} in Fig. 7.

Although C_1 and C_4 are no longer operational, the energy storage unit in zone 1, ES_3 , is capable of providing power to until the load overheats and shuts down at $t\approx 510$ s. The discharging event can be seen in the last two traces in Fig. 7. In particular, note that power remains available to L_3 while the energy stored E_{ES3} decreases, indicating that power is discharged from ES_3 and allocated into L_3 .

The damage to seawater pump SWP_1 also causes a loss of coolant to the component heat exchanger CHX_1 , which provides cooling for G_1 and G_2 . Meanwhile, G_2 remains operational and continue to dissipate heat. The temperature of G_2 , denoted by T_{CHX_1} in Fig. 7, increases until it overheats and shuts down at $t \approx 1960$ s.

In this study, the operability of the IEP is computed to be $O\left(\cdot\right)=0.82$. This example demonstrates the effectiveness of the proposed LPPSS approach as an alternative to direct simulation for early ship design tools. The simulation requires approximately 160 seconds to complete, which is roughly 15 times faster than real time. This approach is also advantageous in that it does not require tuning of the simulation parameters in terms of simulation time steps.

B. Model Comparison

In order to compare and verify the performance of the simplified modeling approach, the system set forth in [2] was considered so that a comparison could be made to a more detailed simulation. The comparison of operability calculations between the two methods is set forth in Table III. Therein, x_d , y_d , and z_d denote the center of the explosion in the Cartesian coordinate. All missile explosions are assumed to have a radius of blast of $r_d = 2.0$ m. Note that

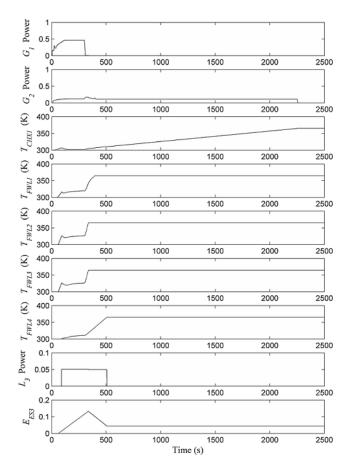


Fig. 7. Time-domain Simulation Results.

TABLE III MODEL COMPARISON

	Event 1	Event 2	Event 3
x_d	100.0 m	38.31 m	39.82 m
y_d	-4.18 m	3.91 m	2.73 m
z_d	3.38 m	2.34 m	3.83 m
Detailed simulation $O(\cdot)$	95.03 %	45.10 %	9.16 %
LPPSS $O(\cdot)$	94.81 %	43.20 %	9.36 %

the operability measures obtained using the LPPSS approach match closely to the operability obtained using a more detailed simulation.

VII. CONCLUSION

A simplified electrical system modeling approach is set forth in this paper. The proposed modeling approach of the electrical system has been demonstrated to reduce the stiffness of the time-domain simulation of the IEP, in order to facilitate early ship design in terms of dependability. The LPPSS method has also been demonstrated to perform reasonably accurate compared to a more detailed simulation. Future works include the optimization of aspects of the ship IEP architecture in terms of component placement to maximize dependability.

ACKNOWLEDGMENT

This work is supported by the Office of Naval Research through Grant N-00014-06-1-0314. It is also supported by the Office of

TABLE IV
LINEAR PROGRAM WEIGHT MATRIX

Index	Weight	Index	Weight
1	1	29	$-\epsilon$
2	3	30	$-\epsilon$
3	2	32	$-\epsilon$
10	0.01	33	$-\epsilon$
11	-0.01	34	$-\epsilon$
12	0.01	35	$-\epsilon$
13	-0.01	37	1
13	0.01	40	1
15	-0.01	46	0.01
22	0.01	47	-0.01
23	-0.01	48	0.01
24	0.01	49	-0.01
25	-0.01	50	$-\epsilon$
27	$-\epsilon$	51	$-\epsilon$
28	$-\epsilon$	_	_

Naval Research through the Electric Ship Research and Development Consortium, Office of Naval Research Grant N00014-08-0080.

APPENDIX

The indices and the weight of c is listed in Table IV, where $\epsilon = 1.0 \times 10^{-4}$. Other indices that are not listed are zero weighted.

Note that a per unit notation is used throughout the models and the results. The base power is chosen herein as $P_{base}=100~\mathrm{kW}$ and the base energy is $E_{base}=10.0~\mathrm{MJ}$.

The generator parameters are: $P_{rated,G1} = P_{rated,G4} = 0.59$ pu, $P_{rated,G2} = P_{rated,G3} = 0.20$ pu, $P_{max,lr} = 0.05$ pu, $P_{max,sr} = 0.05$ pu, $P_{min,lr} = 0.05$ pu, $P_{min,sr} = 0.05$ pu, $m_{max} = 0.05$, $m_{min} = 0.5$, $P_{nl,max} = 0.12$ pu, $P_{nl,min} = 0.05$ pu, $\tau = 1.0$ s, $\eta = 0.98$, and $T_{max} = 365$ K. The converter parameters are: $\eta_{inc} = 0.95$, $P_{nl} = 0.001$ pu, and $T_{max} = 365$ K. The load parameters are: $\eta = 0.98$ and $T_{max} = 365$ K. The energy storage unit parameters are $E_{max} = 0.15$ pu, $P_{d,max} = 0.05$ pu, $P_{c,max} = 0.05$ pu, $\eta = 0.98$, $\tau_{ES} = 1.0$ s, and $P_{nl} = 0.001$ pu.

REFERENCES

- [1] S.D. Sudhoff, S.D. Pekarek, B.T. Kuhn, S.F. Glover, J. Sauer, D.E. Delisle, "Naval Combat Survivability Testbeds for Investigation of Issues in Shipboard Power Electronics Based Power and Propulsion Systems," proceedings of the IEEE Power Engineering Society Summer Meeting, July 21-25, 2002, Chicago, Illinois, USA.
- [2] Aaron M. Cramer, "Metric Based Design of Integrated Engineering Plants For Robust Performance During Hostile Disruptions," Phd. Thesis, Purdue University, August 2007.
- [3] M. O. Said, "Theory and practice of total ship survivability for ship design," Naval Engineers Journal, vol. 107, pp. 191-203, July 1995.
- [4] J. Hill and R. Steinberg, "Design features for survivability of high speed ships," presented at ASNE Reconfiguration and Survivability Symposium 2005, February 2005.
- [5] R.E. Ball and C.N. Calvano, "Establishing the fundamentals of a surface ship survivability design discipline," *Naval Engineers Journal*, vol. 106, no. 1, pp. 71-74, Jan. 1994
- [6] E.K. Chong and S.H. Zak, An Introduction to Optimization, 2nd Edition, Wiley, 2001.
- [7] W.H. Press, S.A. Teukolsky, W.T. Vetterling, and B.P. Flannery, *Numerical Recipes in C: The Art of Scientific Computing*, 2nd ed. Cambridge: Cambridge University Press, 1992.
- [8] N. Doerry, "Zonal ship design," Naval Engineers Journal, vol. 118, no. 1, pp. 39-53, June 2006.